THE ASTRONOMICAL JOURNAL, 120:1794–1800, 2000 October

ULTRAVIOLET OBSERVATIONS OF THE POWERING SOURCE OF THE SUPERGIANT SHELL IN IC 2574

SUSAN G. STEWART
US Naval Observatory, 3450 Massachusetts Avenue NW, Washington, DC 20392-5420; sgs@aa.usno.navy.mil
AND
FABIAN WALTER
California Institute of Technology, Astronomy Department 105-24, Pasadena, CA 91125; fw@astro.caltech.edu
Received 2000 May 31; accepted 2000 June 28

ABSTRACT

A multiband analysis of the region containing the supergiant H I shell in the nearby dwarf irregular galaxy IC 2574 presents evidence of a causal relationship between a central star cluster, the surrounding expanding H I shell, and secondary star formation sites on the rim of the H I shell. Comparisons of the far-UV (FUV, 1521 Å), optical broad band, Hα, X-ray, and H I morphologies suggest that the region is in an auspicious moment of star formation triggered by the central stellar cluster. The derived properties of the H I shell, the central stellar cluster, and the star-forming regions on the rim support this scenario: The kinematic age of the H I shell is <14 Myr and in agreement with the age of the central stellar cluster derived from the FUV observations (~ 11 Myr). An estimate for the mechanical energy input from supernovae and stellar winds of the central stellar cluster, made from FUV photometry and the derived cluster age, is 4.1×10^{52} ergs, roughly a few times higher than the kinetic energy of the H I shell. The requisite energy input needed to create the H I shell, derived in the "standard" fashion from the H I observations (using the numerical models of Chevalier), is 2.6×10^{53} ergs, which is almost 1 order of magnitude higher than the estimated energy input as derived from the FUV data. Given the overwhelming observational evidence that the central cluster is responsible for the expanding H I shell, this discrepancy suggests that the required energy input is overestimated using the "standard" method. This may explain why some other searches for remnant stellar clusters in giant H I holes have been unsuccessful so far. Our observations also show that stellar clusters are indeed able to create supergiant H I shells, even at large galactocentric radii; a scenario that has recently been questioned by a number of authors.

Key words: galaxies: individual (IC 2574) — galaxies: ISM — ISM: bubbles — ISM: structure — ultraviolet emission

1. INTRODUCTION

High-resolution observations in the 21 cm line of neutral hydrogen (H I) show that the interstellar medium (ISM) of galaxies is shaped in a very complex way by holes and shells, most of which are expanding (M31: Brinks & Bajaja 1986; M33: Deul & den Hartog 1990; Holmberg I: Ott et al. 2000; Holmberg II: Puche et al. 1992; IC 10: Wilcots & Miller 1998; IC 2574: Walter & Brinks 1999; DDO 47: Walter & Brinks 2000). Somewhat arbitrarily, these structures are coined "bubbles" (diameters ≈ 10 pc), "superbubbles" (≈ 200 pc), or "supergiant shells" (≈ 1000 pc, hereafter abbreviated SGSs). In the standard picture (e.g., Weaver et al. 1977; McKee & Ostriker 1977; Chu et al. 1995), these structures are believed to be created by young star-forming regions that supposedly eject a great amount of mechanical energy into the ambient ISM in terms of strong stellar winds and subsequent supernova (SN) explosions. In this picture, the energy input of the massive stars creates a cavity filled with hot ionized gas around the star-forming region—this overpressure drives the expansion of a shell, which then collects the ambient neutral material on its rim. For reviews on this topic, the reader is referred to Tenorio-Tagle & Bodenheimer (1988), van der Hulst (1996), Walterbos & Braun (1996), or Brinks & Walter (1998).

Dwarf galaxies have proven to be ideal targets to study the largest of these structures, the SGSs, because dwarf galaxies have puffed-up H I disks, show almost solid-body rotation, and do not possess spiral density waves. As a result, SGSs can form more easily and are not destroyed prematurely (e.g., as a result of shear). We recently reported the discovery of a particularly interesting SGS in IC 2574 (Walter et al. 1998), which is the target of this study.

Although the standard picture to create these H I structures (SNe and strong stellar winds) certainly sounds appealing, observational evidence for this formation process is surprisingly scarce: only in few cases are massive O and B type stars visible in bubbles or superbubbles (see, e.g., N11: Mac Low et al. 1998, or N44: Kim et al. 1998, both situated in the Large Magellanic Cloud). However, in the case of superbubbles, the ages derived for the stellar populations often do not agree with the kinematic ages derived from the expansion velocities of shell structures. For example, from detailed surveys of the massive stars in LMC superbubbles, Oey (1996) found "high-velocity superbubbles" containing central stellar associations with ages much older than the model kinematic ages.

Also, searches for the remnant stellar associations near the centers of H I cavities have not been particularly successful in the past—the standard picture is, therefore, not without its critics. For example, Rhode et al. (1999) could not detect the expected number of remnant A and F stars (as derived from the H I observations) of the clusters that supposedly created the expanding H I holes in Holmberg II. However, Stewart et al. (2000) detected OB stellar populations interior to several H I holes in Holmberg II using ultraviolet data, a direct tracer of the massive stellar component.

Another frequently used argument against creation of SGSs by stellar associations is the location of some SGSs at large galactocentric radii of a galaxy (where star formation

is not expected to play a dominant role). Also, the largest cavities found seem to surpass reasonable energy estimates based on single stellar clusters.

Since bubbles and superbubbles are often only detected in one or two wavelengths, it is difficult, if not impossible, to make meaningful comparisons with theoretical models. Therefore, in-depth, multiwavelength studies are needed. Here, we focus on the SGS in IC 2574 (§ 2) and present evidence in agreement with the standard picture, that this particular SGS has been created by a massive stellar cluster. This scenario is supported by new far ultraviolet (FUV) observations of this region (§ 3), which allow us to independently derive physical properties, such as energy release and age of the powering stellar cluster of a SGS (§ 4). Some surprising results that also affect the interpretation of other SGSs will be discussed in § 5. The results and their implications are summarized in § 6.

2. THE CASE OF IC 2574–SGS

By presenting new observations of an expanding supergiant shell in the nearby, dwarf galaxy IC 2574 (hereafter referred to as IC 2574–SGS, Walter et al. 1998), we aim to shed new light on the controversy over whether or not stellar clusters can create SGSs. The H I shell has a linear size of about 1000 × 500 pc (∼60″ × 30″) and is expanding at ≈25 km s^{-1}. It is therefore an ideal target to study expansion models since, despite its size, it has not stalled yet (as most of the SGSs in other dwarf galaxies have). The elliptical shape of the H I shell in IC 2574 is indicated in Figure 1. The kinematic age ($t = r/v_{\rm exp}$) based on the observed size and expansion velocity is estimated at 14 Myr. Note that this age is actually an upper limit since the shell was presumably expanding faster in the past. This indicates that the least massive stars that go off as SNe are most probably still present in the central stellar association, since their lifetimes (∼50 Myr) are somewhat longer then the dynamical age of the hole (∼14 Myr, as derived from the H I observations).

Based on our H I observations and using the models of Chevalier (1974), we derive that the energy required to produce the shell must be of order 10^{53} ergs, or the equivalent of about 100 Type II SNe (Walter et al. 1998). Note that, in general, all time and shell formation energy requirements are calculated from H I shell size and expansion velocity (e.g., using Chevalier's equation; see the discussion in Walter & Brinks 1999). However, before we begin interpreting these energies, detailed studies of individual shells must be conducted to insure these calculations make sense. The available high-resolution H I data, as well as the presence of the interior stellar association, renders IC 2574–SGS an ideal target to discern if this commonly used approach is indeed justified.

To do so, we present our analysis of FUV data of IC 2574–SGS, which *for the first time gives us an independent measure* of the age and the total mechanical energy deposited by the central stellar association in a SGS. These numbers can then be directly compared with the energy derived from the H I observations.

3. OBSERVATIONS

3.1. *FUV Observations*

The FUV observations were obtained by the Ultraviolet Imaging Telescope (UIT) during the Astro-2 mission using the broadband UIT B1 filter ($\lambda_{\rm eff} = 1521$ Å and $\Delta\lambda = 354$ Å). The IC 2574 FUV image has a 623 s exposure time and spatial resolution of roughly 3″. The image was calibrated using *IUE* spectrophotometry of stars observed by the UIT. The FUV magnitudes are computed from FUV flux using $m_{\rm FUV} = -2.5 \log_{10}[F(\rm FUV)] - 21.1$, where F(FUV) is the incident flux in ergs (cm^2 Å s)$^{-1}$. The chief photometric uncertainties are in the form of low-level nonuniformities introduced via the development and digitization processes. Uncertainty in the absolute calibration can lead to uncertainties of up to 10%–15% in the FUV flux. A detailed discussion of the reduction of the UIT data to flux-calibrated arrays is given by Stecher et al. (1997).

A minimal FUV background level ($\mu > 25$ mag arcsec^{-2}) of 0.53 ± 0.1 analog data units (ADUs) is computed by taking the mean of twenty 20 × 20 pixel boxes in areas void of any galaxy or stellar flux. The UIT has limited accuracy at the lowest light levels. The errors in the background levels reflect this intrinsic uncertainty. A wide, vertical stripe appeared in the center of a sizable percentage of the UIT Astro-2 images, including the IC 2574 image. The flaw appeared on the film and was not a result of the digitization process; its origin is unknown. It has been removed by a model that has been constructed in parts of the image void of the galaxy.

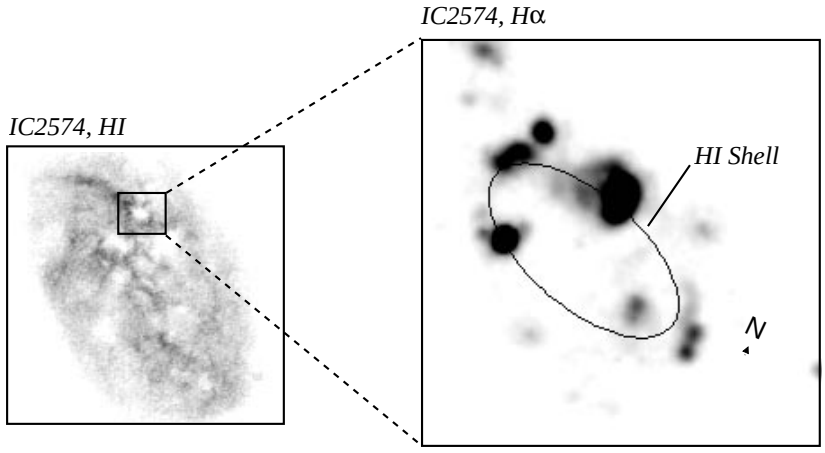

FIG. 1.—*Left*: H I image of IC 2574 with IC 2574–SGS marked. *Right*: Hα image of the central cluster with an ellipse marking the position of the H I shell boundary. The arrow indicates the north direction.

The FUV image presented in Figure 2 (*left*) shows a slight spiral signature suggesting new star formation is preferential to the armlike regions. The enormous complex to the northeast containing IC 2574–SGS (as indicated on the figure) dominates the FUV morphology of the galaxy. This complex alone contributes $\sim 50\%$ of the total integrated FUV flux of IC 2574.

3.2. *Optical Observations*

CCD observations of IC 2574 were obtained in the Johnson *U* and *B* bands, and the Kron-Cousins *R* and Hα bands using the 1.0 m telescope at Mount Laguna Observatory (MLO). The images are median-combined with at least two other images having the same exposure time to remove cosmic rays and other defects. Astrometry and photometry are implemented using standard interactive data language (IDL) procedures for data reduction. The images are calibrated using published photometry of seven stars in the galaxy field (Sandage & Tammann 1974).

The Hα filter at MLO has a centroid wavelength 6573 Å with a width of 61 Å that includes the N II lines. The Hα image is calibrated using fluxes of 20 clearly defined H II regions provided by Miller & Hodge (1994). An Hα emission image is produced by scaling stars in the Hα image with those in the *R*-band image and subtracting the stellar continuum component.

3.3. *FUV, Optical, and* H I *Morphology*

The relative FUV, H I, and Hα morphologies of the region containing IC 2574–SGS are illustrated in Figure 2 (*top right*). The FUV emission is coincident with regions corresponding to both the interior of the H I shell and its rim. The central stellar cluster (Fig. 2, *bottom right*), combined with star formation on the shell boundary, suggests the presence of secondary star formation triggered by the expanding H I shell (see, e.g., the models by Elmegreen 1994). Note that Hα emission corresponds to regions on the rim of IC 2574–SGS while no Hα emission is present in its interior. The FUV-band traces flux from an evolving cluster for longer timescales (roughly 100 Myr) compared with the Hα (roughly a few megayears). Figure 2, therefore, already indicates that the central cluster is relatively older than the star formation on the shell boundary (see also § 4.1).

This situation, as well as the presumed presence of hot X-ray gas in the center of the SGS (Walter et al. 1998), makes IC 2574–SGS a truly unique region and suggests that we have caught this SGS in an auspicious moment. The morphology of the various wavelengths discussed above suggests that this central stellar association is the powering source for the formation and expansion of the shell, as well as for the heating of the X-ray gas. However, this evidence is as yet only circumstantial. Therefore, we present some physical properties of the cluster/shell in the following analysis.

4. ANALYSIS OF THE DATA

4.1. *Age Analysis of IC 2574–SGS*

We estimate the ages of the single regions on the rim of IC 2574–SGS, as well as the central stellar association, from their FUV, *B*, and Hα fluxes. A similar approach is used to characterize the ages of star-forming regions in the dwarf

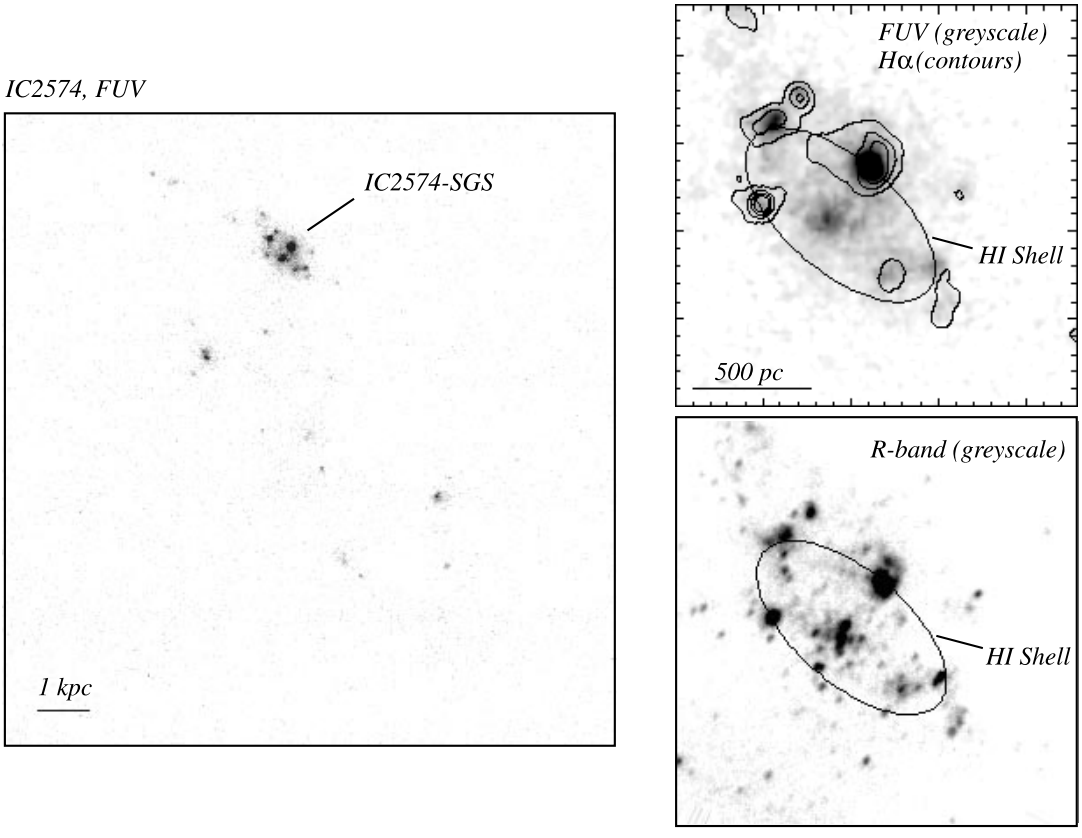

FIG. 2.—*Left*: FUV image of IC 2574 (same region as Fig. 1, *left*). *Top right*: FUV image of the central cluster with an ellipse marking the H I shell boundary (same region as Fig. 1, *right*). The contours represent 5%, 15%, 30%, and 50% of the peak Hα brightness. *Bottom right*: The *R*-band image of the central cluster with an ellipse marking the H I shell boundary. The orientation is the same as in Fig. 1.

irregular Holmberg II by Stewart et al. (2000), where it is described in full detail. Circular apertures are used to identify areas of associated FUV and Hα flux with the aid of a FUV, Hα difference image, shown in Figure 3. The 12 regions are defined by selecting the circular aperture enclosing as much of the FUV and Hα emission from a single region as possible. This rather loose criterion obviously neglects to include all the associated flux from a single region and has the potential to mix regions of different populations, but it is sufficient to discern the relative ages of star formation regions (see Stewart et al. 2000 and the references therein).

Listed in Table 1 are the blue magnitude (m_B), the Hα flux, the FUV flux, and the FUV magnitude ($m_{\rm FUV}$) for each region. Values are corrected for Galactic foreground extinction. Also given in Table 1 are the FUV$-B$ color ($m_{\rm FUV} - m_B$) and $\log(N_{\rm Lyc}/{\rm FUV})$. The latter quantity is the logarithmic ratio of the number of Lyman continuum photons, converted from Hα flux, assuming case B recombination, to FUV flux (where $N_{\rm Lyc}/{\rm FUV} = [F({\rm H}\alpha)/3.02 \times 10^{-12} \times 0.453]/F({\rm FUV})$. The FUV$-B$ color and $\log(N_{\rm Lyc}/{\rm FUV})$ are time-dependent quantities that vary over the lifetime of a cluster and can be compared with model values to estimate an age from the observables.

A single-generation instantaneous burst (IB) model, which employs the stellar evolutionary tracks of Schaerer et al. (1993) and the stellar atmosphere models of Kurucz (1992), is used to derive the expected flux from an evolving cluster in an environment similar to that of IC 2574. The model estimates $L_{\rm FUV}$, $N_{\rm Lyc}$, and L_B assuming an initial mass function (IMF) and metallicity. Figures 4 and 5 show the time dependence of the FUV$-B$ color and $\log(N_{\rm Lyc}/{\rm FUV})$ of a model cluster. To illustrate the model dependence on these assumed parameters, we calculate various combinations of IMF and metallicity. Figure 6 shows the time evolution of $\log(N_{\rm Lyc}/{\rm FUV})$ versus FUV$-B$ color for a cluster based on the results of Figures 4 and 5. The figure depicts the model assuming a Salpeter IMF (2.35) and an SMC-like metallicity, $Z/Z_\odot = 0.1$ (as derived for IC 2574 by Miller & Hodge 1996), which is used

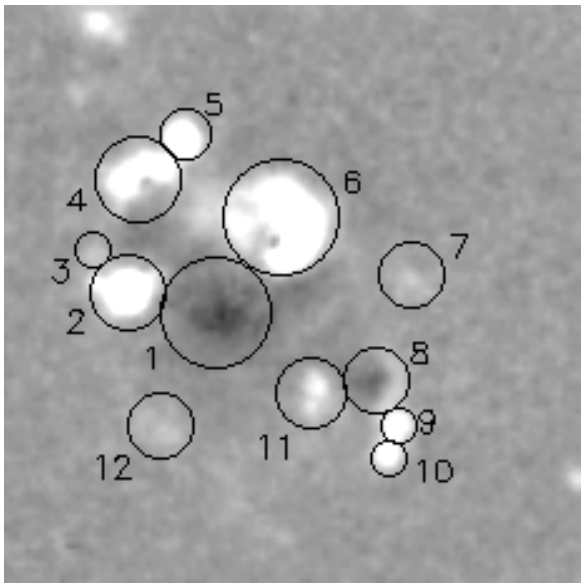

FIG. 3.—FUV, Hα difference image with apertures indicating the regions defined by us. The image is displayed so that areas containing FUV and no Hα are black and areas containing Hα and no FUV are white. The orientation is the same as in Fig. 1.

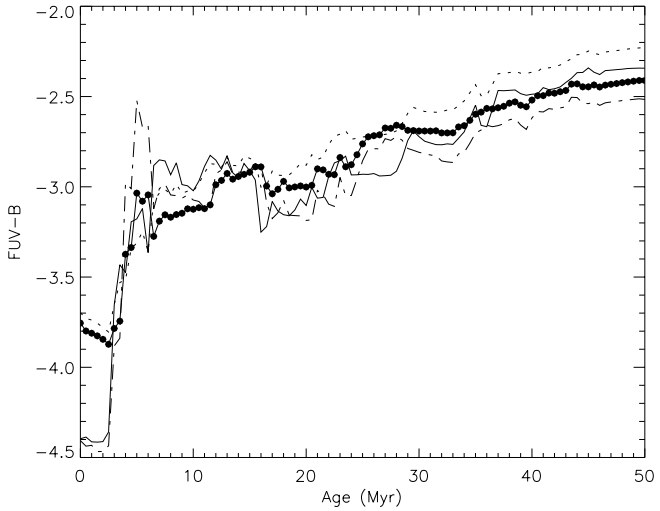

FIG. 4.—Plot illustrating the age dependence of FUV$-B$ color for a single-generation instantaneous burst cluster model. The lines represent a model of LMC metallicity ($Z/Z_\odot = 0.4$) and IMF of 1.08 (*solid line*), a SMC metallicity ($Z/Z_\odot = 0.1$) and IMF of 1.08 (*dash-dotted line*), a LMC metallicity and IMF of 2.35 (*dotted line*), and a SMC metallicity and IMF of 2.35 (*solid line with filled circles*).

TABLE 1

OBSERVATIONS FOR STAR-FORMING REGIONS IN IC 2574–SGS

Region Number	m_B	F(Hα)[a]	F(FUV)[a]	$m_{\rm FUV}$	FUV$-B$	$\log(N_{\rm Lyc}/{\rm FUV})$
1	16.23	13	19.0	13.20	−3.03	11.69
2	17.09	445	5.4	14.57	−2.52	13.78
3	20.25	24	0.8	16.61	−3.64	13.33
4	16.79	296	11.6	13.74	−3.05	13.27
5	18.17	190	3.2	15.15	−3.02	13.64
6	15.68	1000	31.5	12.65	−3.03	13.36
7	18.80	79	2.5	15.42	−3.38	13.37
8	17.83	62	4.8	14.70	−3.13	12.98
9	19.76	71	0.9	16.46	−3.30	13.74
10	19.68	71	0.7	16.72	−2.96	13.84
11	17.61	120	6.0	14.45	−3.16	13.16
12	19.32	55	1.2	16.22	−3.10	13.53

[a] In 10^{-15} ergs (cm^2 Å s)$^{-1}$.

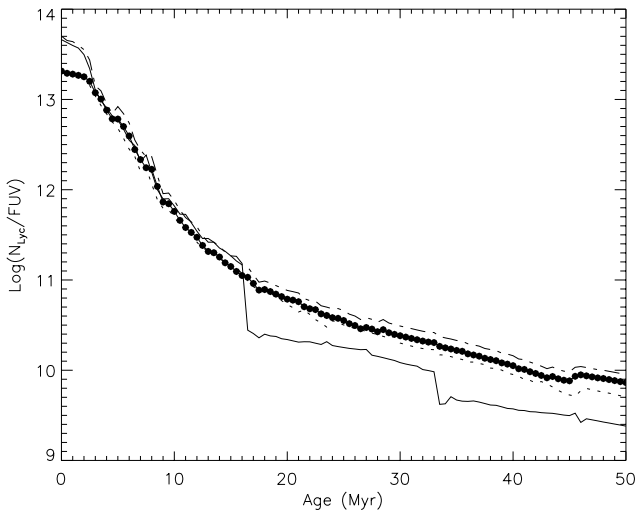

FIG. 5.—Plot illustrating the age dependence of the logarithmic ratio of the number of Lyman continuum photons to FUV flux for a single-generation instantaneous burst cluster model. The lines are the same as for Fig. 3.

in the subsequent derivations. Here, each point represents one age (steps: 0.5 Myr), starting with a 0.5 Myr old cluster in the upper left-hand corner of the graph. The last point on the lower right represents a cluster of an age of 50 Myr.

We use this plot to compare the theoretical model with the actual observed values for FUV$-B$ and $\log(N_{\rm Lyc}/{\rm FUV})$. Since both axes represent time-dependent quantities, the relationship between the observed value and the model is indicative of the age.

Note that most of the observed data points lie off the model, since they are uncorrected for internal extinction.

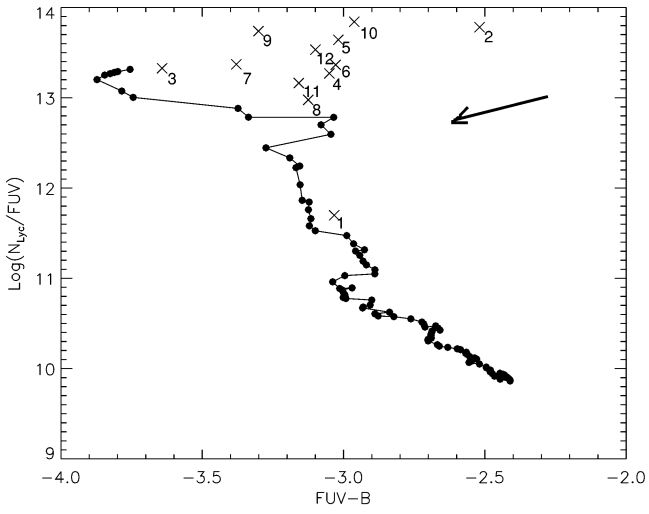

FIG. 6.—The plot of model $\log(N_{\rm Lyc}/{\rm FUV})$ and FUV$-B$ assuming SMC metallicity and Salpeter IMF (based on Figs. 4 and 5). The graph is for a 50 Myr cluster, with each dot representing 0.5 Myr (beginning with a 0.5 Myr old cluster, *upper left-hand corner*). The data points represent the observed values for each region before correction for internal extinction. The subscripts on the data points represent the region numbers (i.e., x_1 = region 1).

Region 1, however (the central stellar cluster; x_1 on the graph), is not far off the theoretical curve. This is not really surprising since we do not expect reddening to play a huge role in this case (since the cluster is situated within the H I cavity). The other regions are obviously still embedded in their parental molecular clouds, which nicely explains the higher reddening.

In order to make an age estimate, the observed FUV$-B$ color and $\log(N_{\rm Lyc}/{\rm FUV})$ are corrected for internal extinction effects. The assumed reddening vector is indicated in the upper right of Figure 6. The SMC reddening curve is used under the assumption that the shape of the curve correlates with metallicity (Verter & Rickard 1998). In the FUV, $A_{\rm FUV}/E(B-V) = 17.72$ (Hill et al. 1997). Each data point is corrected until the point at which it agrees with the theoretical curve. The amount of this correction is an estimate of the internal extinction; the position on the theoretical curve after the correction yields the age of the cluster. The age obtained using this method should be treated as the mean age of stars in the aperture, since a single-generation model is used to interpret flux from what is potentially a mix of populations of slightly different ages. The age estimates are given for each region in Table 2 (col. [1]).

4.2. *Energy Analysis*

The observed FUV flux is used to estimate the mechanical energy imparted to the surrounding ISM of each cluster over its lifetime. The FUV luminosity, $L_{\rm FUV}$, of each region is calculated from the FUV flux after correction for the internal extinction (derived in § 4.1), assuming a distance of 3.2 Mpc (Table 2, col. [2]). The mass of each region is then estimated by comparing the observed $L_{\rm FUV}$ with the model $L_{\rm FUV}$ (ergs s^{-1} $M_\odot^{-1}$) at the cluster's estimated age. The derived masses are given in Table 2 (col. [3]).

Evolutionary synthesis models of populations of massive stars given by Leitherer & Heckman (1995, Fig. 55) provide estimates of the deposition rates, $L_{\rm mech}$, from stellar winds and SNe for an instantaneous burst as a function of time and mass. An average rate of $L_{\rm mech} \sim 2 \times 10^{34}$ ergs (s $M_\odot)^{-1}$ is derived for clusters of similar IMF and metallicity from the models. An estimate of the net mechanical energy deposited into the ISM by SNe and stellar winds, $E_{\rm mech}$, can

TABLE 2

DERIVED PARAMETERS FOR STAR-FORMING REGIONS IN IC 2574–SGS

Region Number	Age (Myr)	$L_{\rm FUV}$ (10^{36} ergs s^{-1})	Mass ($10^3 M_\odot$)	$E_{\rm mech}$ (10^{50} ergs)
1	25.3	25.3	142	412.0
2	33.7	33.7	107	84.5
3	1.3	1.3	4.5	3.0
4	29.7	29.7	113	121.4
5	10.3	10.3	36	23.8
6	94.9	94.9	308	316.1
7	5.3	5.3	16	14.0
8	8.1	8.1	27	32.3
9	2.1	2.1	7.8	4.1
10	2.4	2.4	10	2.7
11	12.0	12.0	39	43.2
12	3.5	3.5	11	8.9

NOTE.—The FUV luminosity is derived from flux corrected for internal extinction and an assumed distance of 3.2 Mpc.

be made by taking the product of $L_{\rm mech}$, the cluster mass, and the cluster age ($E_{\rm mech} \sim L_{\rm mech} \times$ mass $\times$ age). The derived values of $L_{\rm FUV}$ and $E_{\rm mech}$ are given for each cluster in Table 2 (cols. [4] and [5], respectively).

5. DISCUSSION

The analysis of the ages of star-forming regions indicates a dichotomy between the age of the central cluster (region 1) and that of the surrounding regions (regions 2–12). The derived age for the central cluster is $\sim$11 Myr, while the other regions (which all coincide with the rim of the H I shell) range in age from $\sim$1–4.5 Myr (average age: 3.1 Myr). This is also apparent in Figure 6, where the data point for region 1 is found at the lower end of the plot, set off from the rest of the regions. Like the comparison between the FUV and Hα morphologies in Figure 2, our age analysis suggests sequential star formation on the rim of the H I shell, triggered by the expansion of the shell. The age of the central cluster agrees very well with the upper limit derived independently from the H I observations ($\sim$14 Myr). This provides strong independent evidence that the cluster indeed created IC 2574–SGS.

The mechanical energy provided over the lifetime of the central cluster is estimated to be $E_{\rm mech} \sim 4.1 \pm 0.8 \times 10^{52}$ ergs, roughly a factor of 2 times the kinetic energy of the expanding shell, as derived from the H I data ($1.7 \pm 0.5 \times 10^{52}$, Walter et al. 1998). It is now important to compare the total energy estimate based on the FUV observations with previous estimates based on the H I data only. H I–based estimates are usually performed using Chevalier's equation. In the case of IC 2574–SGS, such an energy estimate is 6 times higher than the FUV value ($2.6 \pm 1.0 \times 10^{53}$ ergs, Walter et al. 1998). It is not really surprising that these values do not agree better, since the model by Chevalier is based on the late phase of SNe remnants and simply scaled up to supergiant shells. Our result, therefore, seems to indicate that H I–based energy estimates using Chevalier's equation overestimate the actual energy needed to create an H I shell. This has important consequences for searches for remnant stellar clusters in other SGSs that are based on an expected luminosity of the cluster as derived from the H I data (e.g., Rhode et al. 1999). In other words, if our result holds true for other SGSs as well, one may overestimate the luminosity of a remnant stellar cluster by almost 1 order of magnitude.

6. SUMMARY AND CONCLUSION

A multiband analysis of the region containing the supergiant H I shell in the dwarf galaxy IC 2574 presents evidence of a causal relationship between a central star cluster, a surrounding expanding H I shell, and secondary star formation sites on the rim of the shell.

The key results from the study can be summarized as follows:

1. A stellar cluster interior to the expanding supergiant H I shell in IC 2574 is identified in the FUV and optical bands.
2. The center of the H I shell is void of Hα emission while H II regions coincide with the shell boundary. This is confirmed by the FUV, Hα difference images indicating propagating star formation outward from the center of the shell.
3. A detailed age analysis of the star-forming regions reveals that the central cluster is $\sim$11 Myr and the oldest in the complex. This age agrees very well with the value derived independently from the H I observations (upper limit of $\sim$14 Myr).
4. Analysis of the FUV flux in the central star-forming region indicates that the mechanical energy imparted to the ISM from SNe and stellar winds over the lifetime of the cluster is $\sim 4.1 \pm 0.8 \times 10^{52}$ ergs, roughly a factor of 2 greater than the kinetic energy of the expanding shell.
5. The numerical models of Chevalier suggest an energy input of $2.6 \pm 1.0 \times 10^{53}$ ergs needed to create the H I shell, roughly a factor of 6 greater than the amount of energy input derived using the FUV observations. The fact that the classical method (using the models of Chevalier) seems to overestimate the required energy by almost 1 order of magnitude suggests caution in using it as the basis for determining the required energy input for H I shells. This has important consequences for searches of remnant stellar clusters based on the H I data alone.
6. Our results support the "standard" picture of the creation of supergiant shells by massive star clusters (even at large galactocentric distance). We conclude that a combination of SNe explosions and strong stellar winds are most likely responsible for the supergiant shell in IC 2574.

Our results show that indeed massive stellar clusters can create supergiant shells in galaxies (even at large galactocentric distance) as predicted by the standard picture (creation by SNe explosions and strong stellar winds). One intriguing question remains, of course: why do not we see similar stellar clusters in other supergiant H I shells in IC 2574, as well as in other galaxies? One answer might be that, in the case of IC 2574–SGS, we were just lucky enough to have caught this particular shell in an auspicious moment. We speculate that we may have difficulties detecting the central cluster in IC 2574 after some $\sim 10^8$ yr (a typical age for the largest H I structures found in other galaxies) both because of dimming and dispersion of the cluster stars (since the cluster may not be gravitationally stable after all the gas has been blown away). This would mean that chances to detect similar structures in other galaxies are low, making IC 2574–SGS a truly unique object to study the evolution of supergiant shells in general.

F. W. acknowledges NSF grant AST 96-13717.

REFERENCES

Brinks, E., & Bajaja, E. 1986, A&A, 169, 14
Brinks, E., & Walter, F. 1998, in Proc. Bonn/Bochum-Graduiertenkolleg Workshop, The Magellanic Clouds and Other Dwarf Galaxies, ed. T. Richtler & J. M. Braun (Aachen: Shaker), 1
Chevalier, R. A. 1974, ApJ, 188, 501
Chu, Y.-H., Chang, H.-W., Su, Y.-L., & Mac Low, M.-M. 1995, ApJ, 450, 157
Deul, E. R., & den Hartog, R. H. 1990, A&A, 229, 362
Elmegreen, B. G. 1994, ApJ, 427, 384
Hill, J. K., et al. 1997, ApJ, 477, 673
Kim, S., Chu, Y.-H., Staveley-Smith, L., & Smith, R. C. 1998, ApJ, 503, 729
Kurucz, R. L. 1992, in IAU Symp. 149, Stellar Populations of Galaxies, ed. B. Barbuy & A. Renzini (Dordrecht: Kluwer), 225
Leitherer, C., & Heckman, T. M. 1995, ApJS, 96, 9
Mac Low, M.-M., Chang, T. H., Chu, Y.-H., Points, S. D., Smith, R. C., & Wakker, B. P. 1998, ApJ, 493, 260
McKee, C. F., & Ostriker, J. P. 1977, ApJ, 218, 148
Miller, B. W., & Hodge, P. 1994, ApJ, 427, 656
———. 1996, ApJ, 458, 467
Oey, M. S. 1996, ApJ, 467, 666

Ott, J., Walter, F., Brinks, E., & Klein, U. 2000, AJ, submitted
Puche, D., Westpfahl, D., Brinks, E., & Roy, J.-R. 1992, AJ, 103, 1841
Rhode, K. L., Salzer, J. J., Westpfahl, D. J., & Radice, L. A. 1999, AJ, 118, 323
Sandage, A., & Tammann, G. A. 1974, ApJ, 191, 603
Schaerer, D., Meynet, G., Maeder, A., & Schaller, G. 1993, A&AS, 98, 523
Stecher, T. P., et al. 1997, PASP, 109, 584
Stewart, S. G., et al. 2000, ApJ, 529, 201
Tenorio-Tagle, G., & Bodenheimer, P. 1988, ARA&A, 26, 145
van der Hulst, J. M. 1996, in ASP Conf. Ser. 106, The Minnesota Lectures on Extragalactic Neutral Hydrogen, ed. E. D. Skillman (San Francisco: ASP), 47
Verter, F., & Rickard, L. J. 1998, AJ, 115, 745
Walter, F., & Brinks, E. 1999, AJ, 118, 273
———. 2000, AJ, submitted
Walter, F., Kerp, J., Duric, N., Brinks, E., & Klein, U. 1998, ApJ, 502, L143
Walterbos, R. A. M., & Braun, R. 1996, in ASP Conf. Ser. 106, The Minnesota Lectures on Extragalactic Neutral Hydrogen, ed. E. D. Skillman (San Francisco: ASP), 1
Wilcots, E. M., & Miller, B. W. 1998, AJ, 116, 2363
Weaver, R., McCray, R., Castor, J., Shapiro, P., & Moore, R. 1977, ApJ, 218, 377